# Coincidence site lattice theory of multicrystalline ensembles

**V. Y. Gertsman**

Pacific Northwest National Laboratory, PO Box 999, Richland, WA 99352, USA. Correspondence e-mail: valery.guertsman@pnl.gov

It is shown how the coincidence site lattice theory, developed originally for grain boundaries and extended recently to triple junctions, can be applied to more complex ensembles of crystallites with the cubic crystal structure. These include quadruple points, multiple junctions of grains and other multicrystal assemblies. Application of the theory is demonstrated on hypothetical examples, which may help elucidate some practically important problems.

## 1. Introduction

In a recent paper (Gertsman, 2001), the present author formulated a geometrical theory of triple junctions of grains. It provides a step from our understanding of grain-boundary structure towards a conception of the structure of polycrystals. However, most real polycrystalline materials also contain other types of grain-boundary joints. Thus, if there is more than one layer of grains in the polycrystal, then it must contain grain vertices. The simplest of such objects is the quadruple point, which is the point of contact between four grains and six grain boundaries or, equivalently, the junction of four triple junctions. The quadruple point has nine rotational degrees of freedom (King, 1999) as compared with only three for the grain boundary. Also, quite often multiple junctions of grain boundaries exist, where more than three grains (and grain boundaries) meet along a common line (Kopezky *et al.*, 1991; Gertsman & Szpunar, 1998). An *n*-fold junction has $3(n-1)$ rotational degrees of freedom. Nevertheless, such objects can still be described with the help of the coincidence site lattice (CSL) theory, which was originally developed for grain boundaries (*e.g.* Grimmer *et al.*, 1974). Of course, for the CSL theory to be applicable to crystallite agglomerates, all constituent grain boundaries must have the CSL character.[1] The current paper describes an application of the theory to the grain ensembles built of a limited number of grains having a cubic crystal lattice.

## 2. Σ combination rule for multiple junctions

First, recall that a CSL misorientation between two crystals of the cubic system can be described as (*e.g.* Grimmer *et al.*, 1974)

$$R = \frac{1}{\Sigma}\{a\} = \frac{1}{\Sigma}\begin{pmatrix} a_{11} & a_{12} & a_{13} \\ a_{21} & a_{22} & a_{23} \\ a_{31} & a_{32} & a_{33} \end{pmatrix}, \tag{1}$$

where $\Sigma$ is the reciprocal density of coincident sites and all $a_{ij}$ are co-prime (*i.e.* having no common divisor except 1) integers.

The following theorems describing the combination rules in the junction of three CSL boundaries were proven in the earlier paper (Gertsman, 2001).

Theorem 1:

$$\Sigma_3 = \Sigma_1 \Sigma_2 / \alpha_{12}, \tag{2}$$

where $\alpha_{12}$ is the greatest common divisor (g.c.d.) of the matrix $\{b\} = \{a\}_1\{a\}_2$.

Theorem 2: $\alpha_{12}$ is the square of a common divisor of $\Sigma_1$ and $\Sigma_2$.

Theorem 3: Superposition of three cubic lattices, mutually rotated in such a way that each pair of the lattices creates a CSL, generates a triple-junction CSL with the multiplicity factor

$$\Sigma^{\mathrm{TJ}} = (\Sigma_1 \Sigma_2 \Sigma_3)^{1/2}. \tag{3}$$

In this paper, we formulate the corresponding relationships for the multiple junction.

Theorem 1 is still valid for the multiple junction with the obvious modification (§2.1).

### 2.1. Σ combination rule for a multiple junction

In the *n*-fold junction of *n* CSL boundaries, the reciprocal density of coincident sites for each boundary is calculated as

$$\Sigma_n = \prod_{i=1}^{n-1} \Sigma_i / \alpha_n, \tag{4}$$

where $\alpha_n$ is the g.c.d. of the matrix $\{b\} = \prod_{i=1}^{n-1} \{a\}_i$. (Of course, we can start numeration from any grain boundary, so any boundary can be No. 1 or No. *n*.)

This relationship was proposed by Andreeva and co-workers (Kopezky *et al.*, 1991; Andreeva & Firsova, 1996); however, these authors assumed that at least one of the $\alpha$ values was equal to 1, which is actually not always true. In fact,

---

[1] This notion can be formulated as the requirement that the misorientation axis is rational and the square of the tangent of the rotation angle is a rational number or that the rotation matrix contains only rational elements.

$\alpha \neq 1$ multiple junctions exist as do $\alpha \neq 1$ triple junctions (see Gertsman, 2001).

The proof is analogous to the triple-junction case.

The following equation is valid when all grain orientations are determined in the same reference system:

$$\prod_{i=1}^{n} R_i = I, \tag{5}$$

where $I$ is the identity matrix.

Then,

$$\prod_{i=1}^{n-1} R_i = R_n^T. \tag{6}$$

Here we used the property of cubic (orthonormal) rotations that the inverse and transpose matrices are the same, *i.e.* $R^{-1} = R^T$.

Using (1), we can re-write (6) as

$$\prod_{i=1}^{n-1} \{a\}_i / \Sigma_i = \{a\}_n^T / \Sigma_n. \tag{7}$$

Multiplication of the left-hand side of (7) gives

$$\prod_{i=1}^{n-1} \{a\}_i / \Sigma_i = \{b\} \Big/ \prod_{i=1}^{n-1} \Sigma_i. \tag{8}$$

The components of all matrices $\{a\}_i$ are integers, so $\{b\}$ is an integral matrix. However, it may still be reducible. If $\alpha_n$ is the g.c.d. of $\{b\}$, then from (7) and (8) it follows that $\{a\}_n^T = \{b\}/\alpha_n$ and $\Sigma_n = \prod_{i=1}^{n-1} \Sigma_i/\alpha_n$. ∎

It is easy to see from simple numerical examples (consider *e.g.* a $\Sigma3$–$\Sigma3$–$\Sigma3$–$\Sigma27$ quadruple junction) that Theorem 2 for triple junctions is not valid in the multiple junction case. Instead we have a less restrictive relationship (§2.2).

## 2.2. $\alpha$ theorem for multiple junction

$\alpha_n$ is the square of an integer factor of $\prod_{i=1}^{n-1} \Sigma_i$.

Of course, it is obvious that $\alpha_n$ is an integer factor of $\prod_{i=1}^{n-1} \Sigma_i$, otherwise we cannot obtain integer $\Sigma_n$ [see formula (4) above]. However, it is not so obvious that it must be a square.

Any CSL misorientation can be described by a quaternion of co-prime integers $(k, l, m, n)$ and in the cubic system [see *e.g.* Gertsman (2001) for references]:

$$\Sigma = \text{g.o.f.}(k^2 + l^2 + m^2 + n^2), \tag{9}$$

where g.o.f. stands for 'the greatest odd factor'.

In an $n$-fold junction, the misorientation of each boundary can be calculated through the misorientations of all the other boundaries [see *e.g.* (6) above]. Using the quaternion notation, this can be written as

$$(K, L, M, N) = \prod_{i=1}^{n-1} (k_i, l_i, m_i, n_i). \tag{10}$$

Even though all the generating quaternions contain co-prime coefficients, the product quaternion may still be reducible. Suppose $\beta$ is the greatest common odd divisor of $(K, L, M, N)$. Then,

$$\Sigma_n = \text{g.o.f.}(K^2 + L^2 + M^2 + N^2)/\beta^2. \tag{11}$$

It can be proven using the method of mathematical induction that

$$K^2 + L^2 + M^2 + N^2 = \prod_{i=1}^{n-1} (k_i^2 + l_i^2 + m_i^2 + n_i^2). \tag{12}$$

For $n = 2$, it can be shown by direct calculation [see equation (21) in Gertsman (2001)].

Assume equation (12) is true for $n = k$, *i.e.*

$$K_k^2 + L_k^2 + M_k^2 + N_k^2 = \prod_{i=1}^{k-1} (k_i^2 + l_i^2 + m_i^2 + n_i^2). \tag{13}$$

Let us multiply quaternion $(K_k, L_k, M_k, N_k)$ by quaternion $(k_k, l_k, m_k, n_k)$. According to the quaternion multiplication law [see *e.g.* equation (21) in Gertsman (2001)], the resultant quaternion $(K_{k+1}, L_{k+1}, M_{k+1}, N_{k+1})$ has the following components:

$$\begin{aligned} K_{k+1} &= K_k n_k + N_k k_k + L_k m_k - M_k l_k \\ L_{k+1} &= M_k k_k - K_k m_k + N_k l_k + L_k n_k \\ M_{k+1} &= K_k l_k - L_k k_k + N_k m_k + M_k n_k \\ N_{k+1} &= N_k n_k - K_k k_k - L_k l_k - M_k m_k. \end{aligned} \tag{14}$$

From (14), by direct calculation we obtain

$$\begin{aligned} &K_{k+1}^2 + L_{k+1}^2 + M_{k+1}^2 + N_{k+1}^2 \\ &= (K_k^2 + L_k^2 + M_k^2 + N_k^2)(k_k^2 + l_k^2 + m_k^2 + n_k^2). \end{aligned} \tag{15}$$

Substituting (13) in (15) yields

$$(K_{k+1}^2 + L_{k+1}^2 + M_{k+1}^2 + N_{k+1}^2) = \prod_{i=1}^{k} (k_i^2 + l_i^2 + m_i^2 + n_i^2), \tag{16}$$

which proves (12).

Now, from (9) and (12), we obtain

$$\begin{aligned} \prod_{i=1}^{n-1} \Sigma_i &= \prod_{i=1}^{n-1} \text{g.o.f.}(k_i^2 + l_i^2 + m_i^2 + n_i^2) \\ &= \text{g.o.f.} \prod_{i=1}^{n-1} (k_i^2 + l_i^2 + m_i^2 + n_i^2) \\ &= \text{g.o.f.}(K^2 + L^2 + M^2 + N^2). \end{aligned} \tag{17}$$

From (11) and (17), we find $\Sigma_n = \prod_{i=1}^{n-1} \Sigma_i/\beta^2$. ∎

## 3. CSL multiplicity factor for multicrystals

Obviously, a lattice of common sites (multi-CSL) can be formed by superposition of more than three misoriented crystal lattices. However, if $n > 3$, then for the same set of crystal orientations different combinations of grain-boundary CSLs are possible. The multi-CSL depends on the mutual orientations of constituent crystallites, but not on how they are spatially arranged and connected to each other. That is, the same multi-CSL describes multiple junctions and multicrystals with different spatial arrangements of grains and boundaries if the set of crystallite orientations is the same for each configuration. Because of that, the procedure of finding the

reciprocal density of coincident sites of the multi-CSL is more of an algorithm than a simple analytical formula. The following relationship is suggested:

$$\Sigma^{\text{multi}} = \text{g.c.d.} \left( \prod_{i=1}^{n} \Sigma_i \right)_k^{1/2}, \qquad (18)$$

where $\left( \prod_{i=1}^{n} \Sigma_i \right)_k$ represents all $k$ possible multiple junction arrangements of the given crystal orientations.

Relationship (18) is introduced here as a conjecture and not a theorem because some propositions used for its derivation are yet to be rigorously proven. Below we show how this relationship can be substantiated.

First, one can see that Theorem 3 of Gertsman (2001), see equation (3) above, satisfies relationship (18) since $k = 1$ for the triple junction and g.c.d.$(\Sigma_1 \Sigma_2 \Sigma_3)^{1/2} = (\Sigma_1 \Sigma_2 \Sigma_3)^{1/2}$.

Let us analyse a quadruple junction or a tetracrystal. Recall (Miyazawa et al., 1996; Gertsman, 2001) that, for a triple junction of CSL boundaries,

$$\Sigma_1 = pq, \quad \Sigma_2 = qr, \quad \Sigma_3 = pr, \qquad (19)$$

where $p$, $q$, $r$ are positive odd integers.

Consider two adjacent CSL triple junctions sharing one grain boundary (Fig. 1). Let (19) describe the $A$–$B$–$C$ junction, and for the $A$–$C$–$D$ junction a similar relationship can be written:

$$\Sigma_3 = tu, \quad \Sigma_4 = st, \quad \Sigma_5 = su, \qquad (20)$$

where $s$, $t$, $u$ are again positive odd integers.

Since $pr = tu$, these four integers can be represented as[2]

$$p = p_1 p_2, \quad r = r_1 r_2, \quad t = p_1 r_1, \quad u = p_2 r_2, \qquad (21)$$

where $p_1$, $p_2$, $r_1$, $r_2$ are positive odd integers.

Similarly, if we embed a triangular crystal with orientation $D$ into the $A$–$B$–$C$ tricrystal (Fig. 2a), the corresponding grain-boundary $\Sigma$'s can be represented as follows:

$$\begin{aligned} \Sigma_1 &= p_1 p_2 q_1 q_2, & \Sigma_2 &= q_1 q_2 r_1 r_2, & \Sigma_3 &= p_1 p_2 r_1 r_2, \\ \Sigma_4 &= p_2 q_1 r_2 s, & \Sigma_5 &= p_2 q_2 r_1 s, & \Sigma_6 &= p_1 q_2 r_2 s. \end{aligned} \qquad (22)$$

Again, all the factors here are positive odd integers.

The crystallite arrangement in Fig. 2(a) contains all six grain boundaries[3] and four triple junctions (one of which, $A$–$B$–$C$, is a virtual junction) that the four given crystal orientations can form. The other three configurations in Fig. 2 contain the same elements. Crystallites with four different crystal orientations can also form three quadruple junctions (Fig. 3).

Arguments analogous to Theorem 3 of Gertsman (2001) lead to the conclusion that the reciprocal density of coincident sites of the multi-CSL of the four crystals is given by

$$\Sigma^{\text{tetra}} = p_1 p_2 q_1 q r_1 r_2 s = pqrs. \qquad (23)$$

Let us calculate the $\Sigma$ products for the quadruple junctions (see Fig. 3):

---

[2] Miyazawa et al. (1996) have implied that it is always the case that $p = t$ and $r = u$ (see Fig. 1 in their paper). Therefore, a number of possible combinations of $\Sigma$ values is missing in their Table 2.
[3] Remember that grain-boundary planes are not included in our analyses and grain joints are characterized entirely by crystallite misorientations.

$$\Sigma_1 \Sigma_2 \Sigma_5 \Sigma_6 = p_1^2 p_2^2 q_1^2 q_2^4 r_1^2 r_2^2 s^2 = (q_2 \Sigma^{\text{tetra}})^2 \qquad (24a)$$

$$\Sigma_1 \Sigma_3 \Sigma_4 \Sigma_5 = p_1^2 p_2^4 q_1^2 q_2^2 r_1^2 r_2^2 s^2 = (p_2 \Sigma^{\text{tetra}})^2 \qquad (24b)$$

$$\Sigma_2 \Sigma_3 \Sigma_4 \Sigma_6 = p_1^2 p_2^2 q_1^2 q_2^2 r_1^2 r_2^4 s^2 = (r_2 \Sigma^{\text{tetra}})^2. \qquad (24c)$$

Equations (24) correspond to relationship (18) if

$$\text{g.c.d.}(p_2, q_2, r_2) = 1. \qquad (25)$$

Suppose it is not so, i.e.

$$\text{g.c.d.}(p_2, q_2, r_2) = x \neq 1, \quad p_2 = xp_2', \quad q_2 = xq_2', \quad r_2 = xr_2'. \qquad (26)$$

Introduce

$$p_1' = xp_1, \quad q_1' = xq_1, \quad r_1' = xr_1, \quad s' = xs. \qquad (27)$$
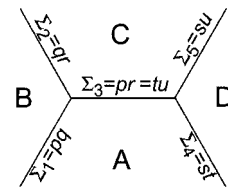


**Figure 1**
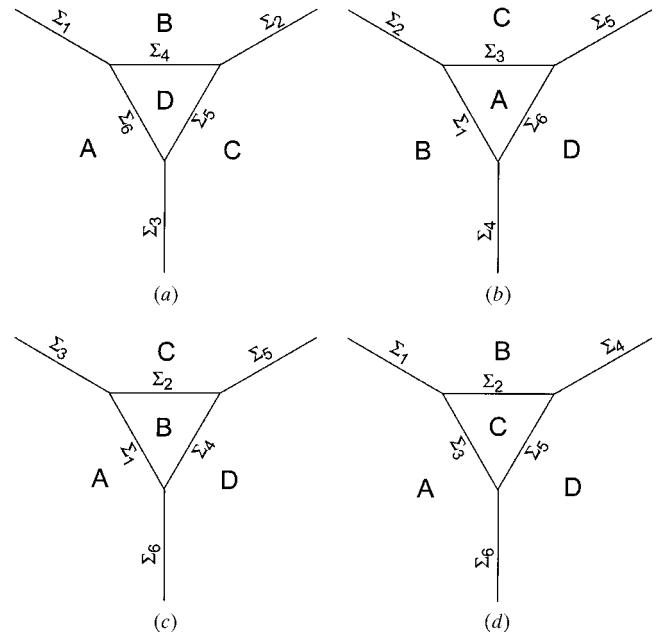Two adjacent triple junctions of CSL boundaries.



**Figure 2**
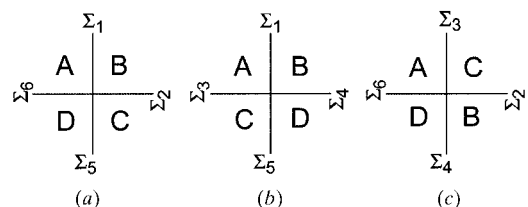Tetracrystals with maximum number of triple junctions.



**Figure 3**
Three possible quadruple junctions with the same crystal orientations of the four crystallites.

Then,

$$\Sigma_1 = p_1'p_2'q_1'q_2', \quad \Sigma_2 = q_1'q_2'r_1'r_2', \quad \Sigma_3 = p_1'p_2'r_1'r_2',$$
$$\Sigma_4 = p_2'q_1'r_2's', \quad \Sigma_5 = p_2'q_2'r_1's', \quad \Sigma_6 = p_1'q_2'r_2's'. \quad (28)$$

This would mean that the representation (22) of the six $\Sigma_i$ by the factors $p_1, p_2, \ldots, s$ is not unique, which is, apparently, not true.[4] Then, $x = 1$ and (18) is valid.

Now, consider what occurs if a fifth crystallite is added to the system. For example, take the quadruple junction shown in Fig. 3(a) with grain boundaries characterized by $\Sigma_1, \Sigma_2, \Sigma_5, \Sigma_6$ [see (22)] and embed crystal $E$ into it (Fig. 4). The new grain-boundary misorientations can be represented as

$$\Sigma_7 = p_2q_1r_1t, \quad \Sigma_8 = p_2q_2r_2t, \quad \Sigma_9 = r_1r_2st, \quad \Sigma_{10} = p_1q_2r_1t. \quad (29)$$

In this case,

$$\Sigma^{\text{penta}} = p_1p_2q_1qr_1r_2st = pqrst. \quad (30)$$

Calculations (omitted here to save space) of the $\Sigma$ products for all 12 possible quintuple junctions again confirm relationship (18).

Evidently, an addition of a new crystal orientation to the system appends a new (positive odd) factor to $\Sigma^{\text{multi}}$. Thus, for an ensemble of $n$ crystallites,

$$\Sigma^{\text{multi}} = \prod_{i=1}^{n} m_i, \quad (31)$$

where $m_i$ are divisors of grain-boundary $\Sigma$'s.

Apparently, relationship (18) is then valid for any $n$. Any multicrystal can be topologically transformed into a multiple junction: a continuous chain of grain boundaries can shrink into a common line, thus reducing a multicrystal or grain cluster to a multiple junction. Of course, the number of misorientations $n$ in each case is equal to the number of different crystal orientations in the system.

Let us check on a concrete example how the algorithm works. Consider four crystals having the following orientations (all are expressed in the coordinate system of crystal $A$):

$$A = \begin{pmatrix} 1 & 0 & 0 \\ 0 & 1 & 0 \\ 0 & 0 & 1 \end{pmatrix}, \quad B = \frac{1}{3}\begin{pmatrix} 2 & 1 & -2 \\ 1 & 2 & 2 \\ 2 & -2 & 1 \end{pmatrix},$$

$$C = \frac{1}{27}\begin{pmatrix} 25 & 2 & -10 \\ 2 & 25 & 10 \\ 10 & -10 & 23 \end{pmatrix}, \quad D = \frac{1}{9}\begin{pmatrix} 8 & 1 & 4 \\ 1 & 8 & -4 \\ -4 & 4 & 7 \end{pmatrix}. \quad (32)$$

One can easily find that mutual misorientations between the crystals are:

$$R_{AB} = \Sigma 3, \quad R_{AC} = \Sigma 27a, \quad R_{AD} = \Sigma 9,$$
$$R_{BC} = \Sigma 9, \quad R_{BD} = \Sigma 3, \quad R_{CD} = \Sigma 3. \quad (33)$$

---

[4] If this statement were proven and not introduced as a proposition, then equation (18) would be proven as a theorem, at least for the case $n = 4$.

The solution of relationships (22) in this case is $p_1 = 3$, $p_2 = 1$, $q_1 = 1$, $q_2 = 1$, $r_1 = 3$, $r_2 = 3$, $s = 1$. Then, from (23), $\Sigma^{\text{tetra}} = 27$. Fig. 5 displays possible planar arrangements of the four crystallites. Note that the configurations in the second and third columns topologically represent parts of the configurations shown in Fig. 2. Calculating $(\prod_{i=1}^{n} \Sigma_i)^{1/2}$ for the quadruple junctions in Figs. 5(a),(d),(g) gives 27, 27 and 81, respectively. Therefore, the rule expressed by relationship (18) is satisfied. That the superposition of the four given crystal lattices produces a multi-CSL with $\Sigma = 27$ is evident, e.g. from Fig. 5(c); the CSL of boundary $A/C$ coincides with the triple-junction CSLs of junctions $A$–$B$–$C$ and $A$–$C$–$D$, i.e. it is a common sublattice of all the four crystal lattices. Consideration of other numerical examples, including crystallite arrangements with $n > 4$ as well as with $\alpha \neq 1$ triple junctions confirms the algorithm for finding the multiplicity factor expressed by equation (18).
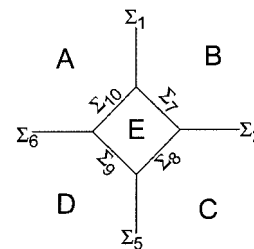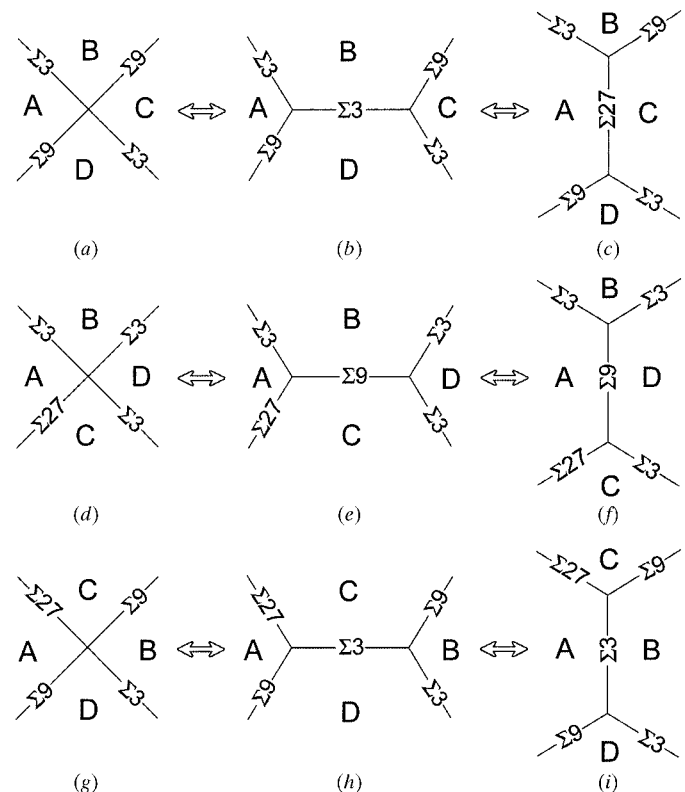


**Figure 4**
Pentacrystal.



**Figure 5**
Planar arrangements of four crystallites producing three $\Sigma 3$, two $\Sigma 9$ and one $\Sigma 27$ misorientation.

It is possible to formally introduce the CSL of the poly-crystal with the multiplicity factor calculated according to relationships (18) and (31). Of course, in most practical cases, $\Sigma^{multi}$ would be an astronomical number. However, this concept might be useful in some special cases, such as certain grain clusters or specially prepared thin-film structures. For example, hypothetically one can fabricate a polycrystalline film with only three different orientations of crystallites. Let us take the following three crystal orientations:

$$A = \begin{pmatrix} 1 & 0 & 0 \\ 0 & 1 & 0 \\ 0 & 0 & 1 \end{pmatrix}, \quad B = \frac{1}{3}\begin{pmatrix} 2 & 1 & -2 \\ 1 & 2 & 2 \\ 2 & -2 & 1 \end{pmatrix},$$
$$C = \frac{1}{3}\begin{pmatrix} 1 & 2 & -2 \\ 2 & 1 & 2 \\ 2 & -2 & -1 \end{pmatrix}. \tag{34}$$

Then, the misorientations between the crystals are:

$$R_{AB} = \Sigma3, \quad R_{AC} = \Sigma3, \quad R_{BC} = \Sigma9. \tag{35}$$

A schematic of the two-dimensional microstructure built of such crystallites is shown in Fig. 6. For simplicity, it is drawn consisting of regular hexagons. The grain shapes are not important, but it is essential that there are only triple junctions in the network. The triple junctions in this microstructure correspond to the case considered in Fig. 5 of Dimitrakopulos & Karakostas (1996). It is easy to see that this polycrystal has $\Sigma^{multi} = 9 \; (= \Sigma^{GB} = 9)$.

Miyazawa *et al.* (1996) have suggested another variant of a two-dimensional network built of only $\Sigma3$ and $\Sigma9$ grain boundaries. The four constituent orientations can be represented as
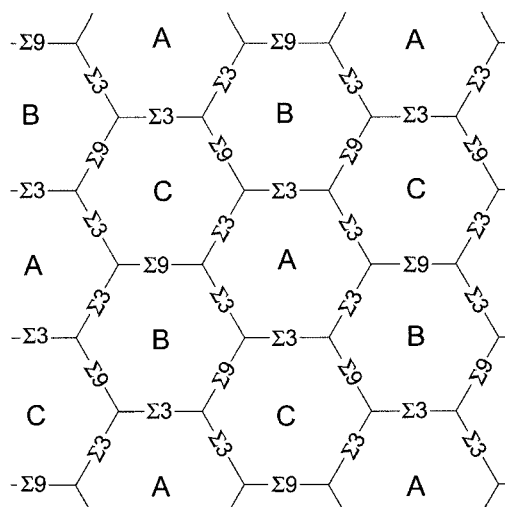
$$A = \begin{pmatrix} 1 & 0 & 0 \\ 0 & 1 & 0 \\ 0 & 0 & 1 \end{pmatrix} \quad B = \frac{1}{3}\begin{pmatrix} -1 & 2 & 2 \\ 2 & -1 & 2 \\ 2 & 2 & -1 \end{pmatrix}$$
$$C = \frac{1}{3}\begin{pmatrix} -1 & 2 & -2 \\ 2 & -1 & -2 \\ -2 & -2 & -1 \end{pmatrix} \quad D = \frac{1}{3}\begin{pmatrix} -1 & -2 & 2 \\ -2 & -1 & -2 \\ 2 & -2 & -1 \end{pmatrix}. \tag{36}$$

The misorientations between the crystallites are

$$R_{AB} = \Sigma3, \quad R_{AC} = \Sigma3, \quad R_{AD} = \Sigma3,$$
$$R_{BC} = \Sigma9, \quad R_{BD} = \Sigma9, \quad R_{CD} = \Sigma9. \tag{37}$$

The only triple junctions possible in the network built of these crystallites are $\Sigma3$–$\Sigma3$–$\Sigma9$ and $\Sigma9$–$\Sigma9$–$\Sigma9$ [see *e.g.* Fig. 2 of Miyazawa *et al.* (1996) as an illustration]. For such a network, $\Sigma^{multi} = 27 \; (= \Sigma^{TJ} = 27)$.

It is possible to construct other two-dimensional networks having only $\Sigma3$ and $\Sigma9$ boundaries. An example is shown in Fig. 7. Its principal difference from the microstructure presented in Fig. 6 is that there are four different crystallite orientations, which could be represented *e.g.* in form (32). One of the mutual misorientations in this case is $\Sigma27a$ [see (33)], but there are no such boundaries in the microstructure because crystallites with orientations $A$ and $C$ are nowhere adjacent. The triple junctions in this microstructure correspond to the case considered in Fig. 8 of Dimitrakopulos & Karakostas (1996). It is certainly possible to generate $\Sigma27a$ grain boundaries in this network by simple topological transformations. The microstructure in Fig. 7 (and all others obtained from it by transformations retaining the four crystal orientations) can be described by $\Sigma^{multi} = 27 \; (= \Sigma^{GB} = 27a)$.

## 4. Analysis of quadruple point

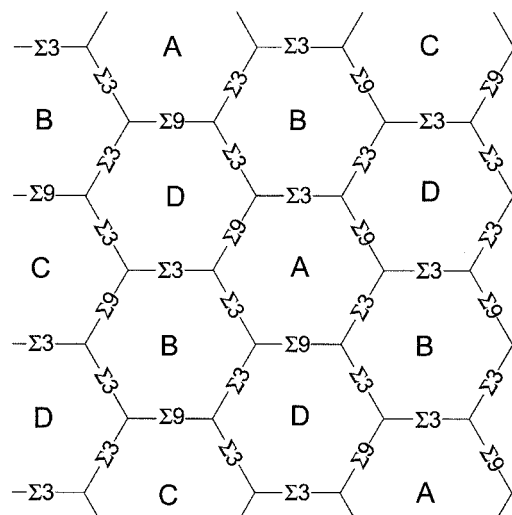When considering a common CSL, the crystallite assemblage does not necessarily have to be two-dimensional. Thus, the



**Figure 6**
Two-dimensional network of $\Sigma3$ and $\Sigma9$ boundaries with $\Sigma^{multi} = 9$.



**Figure 7**
Two-dimensional network of $\Sigma3$ and $\Sigma9$ boundaries with $\Sigma^{multi} = 27$

same relationships (18) and (31) are applicable to grain vertices. Here we analyse a practically important example of such a vertex, the quadruple point (Fig. 8). Six grain boundaries meet at such a point but the misorientations of only three of them are independent. Assume that the misorientations of three boundaries are known, *e.g.* $A/D$ is described by $\Sigma_6$, $B/D$ by $\Sigma_4$ and $C/D$ by $\Sigma_5$ ($A$, $B$, $C$ being the three 'top' crystallites and $D$ the 'bottom' grain, see Fig. 8). Of course, it is not essential which misorientations are specified. What is essential is that the given independent misorientations do not belong to the same triple junction because in this case only two of them would be independent. Given the three misorientations, one can calculate the remaining three because each of the four triple junctions contains a pair of the specified boundaries. Thus, $\Sigma$ values are determined through relationship (2), *i.e.* for misorientations $A/B$, $B/C$ and $A/C$, respectively, we have:

$$\Sigma_1 = \Sigma_4\Sigma_6/\alpha_{46}, \quad \Sigma_2 = \Sigma_4\Sigma_5/\alpha_{45}, \quad \Sigma_3 = \Sigma_5\Sigma_6/\alpha_{56}. \quad (38)$$

One can notice that the two-dimensional schematics shown above in Fig. 2 can be used to represent planar sections of the quadruple point arrangement of the four crystallites. For example, a section perpendicular to the $A$–$B$–$C$ triple junction made below the quadruple point gives the configuration shown in Fig. 2(*a*). Hence, relationships (22) can be used to represent the $\Sigma$'s of the grain boundaries forming the quadruple point.

Consider transformations of the quadruple point into orientationally equivalent quadruple junctions. The transformation consists in cutting a wedge in the $A$–$B$–$C$ tricrystal and replacing it with a wedge-shaped crystal having the $D$ orientation. Fig. 3 above may serve as an illustration of the three topologically possible variants. The $(\prod_{i=1}^{n} \Sigma_i)^{1/2}$ values for these variants are

$$(\Sigma_1\Sigma_2\Sigma_5\Sigma_6)^{1/2} = \Sigma_4\Sigma_5\Sigma_6/(\alpha_{45}\alpha_{46})^{1/2} \quad (39a)$$

$$(\Sigma_1\Sigma_3\Sigma_4\Sigma_5)^{1/2} = \Sigma_4\Sigma_5\Sigma_6/(\alpha_{46}\alpha_{56})^{1/2} \quad (39b)$$

$$(\Sigma_2\Sigma_3\Sigma_4\Sigma_6)^{1/2} = \Sigma_4\Sigma_5\Sigma_6/(\alpha_{45}\alpha_{56})^{1/2}. \quad (39c)$$

The CSL multiplicity factor of the quadruple point, $\Sigma^{QP}$, is given by the g.c.d. of the three integers expressed by equations (39). Note that the right-hand parts of equations (39) contain only the parameters describing grain boundaries $A/D$, $B/D$ and $C/D$. That is, $\Sigma^{QP}$ is fully determined by the 'pyramidal'
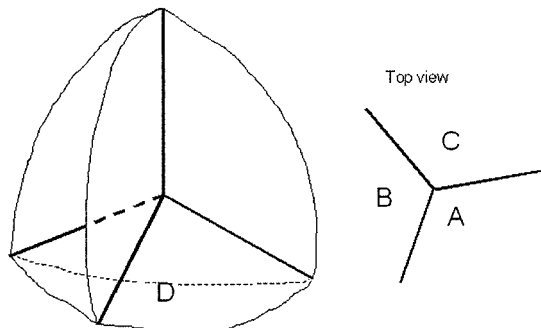


**Figure 8**
Quadruple point.

grain boundaries, *i.e.* the boundaries of the same crystallite having a common vertex. Of course, any one of the four pyramidal groups of boundaries forming the quadruple point can be used for calculations.

As an example, let us construct a quadruple point comprising only $\Sigma 3$ and $\Sigma 9$ grain boundaries. Assume that the boundaries in Fig. 8 have the following misorientations: $A/D$, $B/D$ and $C/D$, all $\Sigma = 3$. Then, from (38), boundaries $A/B$, $B/C$ and $A/C$ all have misorientations $\Sigma = 9$. Thus, three $\Sigma 3$ and three $\Sigma 9$ boundaries meet in this quadruple point. In this case, $p_1 = 3, p_2 = 1, q_1 = 3, q_2 = 1, r_1 = 3, r_2 = 1, s = 1$. Any method of calculation gives the multiplicity factor for the quadruple point CSL $\Sigma^{QP} = 27$. A hypothetical polycrystal built of Kelvin's tetrakaidecahedra presented in Fig. 6 of Miyazawa *et al.* (1996) have only four different crystal orientations and contains only the quadruple points of the type we have just considered. In that case, $\Sigma^{multi} = 27$ for the whole polycrystal.

It is also possible to have a quadruple point having all six $\Sigma 9$ boundaries. In this case, $\Sigma^{QP} = 81$.

At first glance, it seems that it is also possible to assemble four $\Sigma 3$ and two $\Sigma 9$ boundaries in a quadruple point. However, if the two $\Sigma 9$ boundaries belonged to the same triple junction, then relationships expressed by (2) would not be satisfied for all four triple junctions in the system, since there would be two impossible triplets: $\Sigma 3$–$\Sigma 3$–$\Sigma 3$ and $\Sigma 3$–$\Sigma 9$–$\Sigma 9$. Then it looks as if the following combination is possible. Suppose that boundaries $A/D$ and $B/C$ in Fig. 8 have $\Sigma = 9$ and all the others $\Sigma = 3$. In this case, each triple junction considered separately seems to satisfy relationship (2). However, four different crystal orientations cannot form four $\Sigma 3$ and two $\Sigma 9$ misorientations. The maximum number of $\Sigma 3$ misorientations formed by four different orientations is three, with two $\Sigma 9$s and one $\Sigma 27$. Relationships (32) and (33) represent a variant with the $\Sigma 27a$ grain-boundary misorientation. A variant containing $\Sigma 27b$ can be represented for example by the following crystal orientations:

$$A = \begin{pmatrix} 1 & 0 & 0 \\ 0 & 1 & 0 \\ 0 & 0 & 1 \end{pmatrix}, \qquad B = \frac{1}{3}\begin{pmatrix} 2 & 2 & -1 \\ 2 & -1 & 2 \\ 1 & -2 & -2 \end{pmatrix},$$

$$C = \frac{1}{27}\begin{pmatrix} 26 & 2 & 7 \\ 2 & 23 & -14 \\ -7 & 14 & 22 \end{pmatrix}, \quad D = \frac{1}{9}\begin{pmatrix} 7 & 4 & 4 \\ 4 & 1 & -8 \\ -4 & 8 & -1 \end{pmatrix},$$

$$(40)$$

with the following misorientations between the crystals:

$$\begin{array}{llll} R_{AB} = \Sigma 3, & R_{AC} = \Sigma 27b, & R_{AD} = \Sigma 9, \\ R_{BC} = \Sigma 9, & R_{BD} = \Sigma 3, & R_{CD} = \Sigma 3. \end{array} \quad (41)$$

Figs. 5 and 7 can still serve as schematics for this variant. The only possibility to have only $\Sigma 3$ and $\Sigma 9$ misorientations in proportion 2:1 is to have just three crystal orientations, as in Fig. 6. However, it is impossible to build a three-dimensional microstructure out of three crystal orientations. Hence, the

quadruple point consisting of four $\Sigma 3$ and two $\Sigma 9$ boundaries is impossible.

This apparently minor conclusion may have a rather important implication for the grain-boundary engineering approach (*e.g.* Watanabe, 1984). This term stands for the manipulation of the polycrystal properties through altering the grain-boundary distribution. The ultimate goal is to create such a set of grain boundaries that would resist damage propagation (such as cracking and corrosion) along the grain-boundary network. The proportion and spatial arrangement of damage-resistant boundaries are of primary importance for this. Palumbo *et al.* (1992) proposed that the 'theoretical limit' for the fraction of $\Sigma 3$ boundaries, which are supposedly the most damage resistant, in the polycrystal is 2/3, and this figure has been used in the subsequent models. The 2/3 limit is based on the consideration of the triple junction as the building block of the polycrystal and it has been projected to the three-dimensional case as well. However, this is true only for virtually two-dimensional microstructures, examples of which are presented in Figs. 6 and 7. The quadruple point should be considered as the smallest element retaining three-dimensional polycrystalline properties. The examples analyzed above demonstrate that the fraction of $\Sigma 3$ boundaries in the three-dimensional polycrystal cannot exceed $\frac{1}{2}$ (if there are no $n > 3$ junctions).[5] Furthermore, if the $4 \times \Sigma 3 + 2 \times \Sigma 9$ quadruple point were possible, then the two $\Sigma 9$ boundaries in it would be connected only at one point. The above analysis shows, however, that there should be a continuous surface of $\Sigma 9$ boundaries in the three-dimensional polycrystal [see *e.g.* Fig. 6 of Miyazawa *et al.* (1996) as an illustration]. Recent

experimental study (Gertsman & Bruemmer, 2001) has shown that, while $\Sigma 3$ boundaries are resistant to intergranular stress corrosion cracking in many practically important materials, $\Sigma 9$ boundaries are not. Therefore, having a continuous surface of $\Sigma 9$ boundaries may be detrimental since they could provide easy paths for intergranular damage propagation even if the 'twin-limited' microstructure with the maximum possible proportion of $\Sigma 3$ boundaries were attained. Hence, the primary goal of grain-boundary engineering should be understanding the lack of damage resistance of the $\Sigma 9$ boundary.

---

[5] The presence of multiple junctions can, of course, increase the proportion of $\Sigma 3$ boundaries above the 'theoretical limit', as discussed by Gertsman & Szpunar (1998).

## References

Andreeva, A. V. & Firsova, A. A. (1996). *Mater. Sci. Forum*, **207–209**, 189–192.
Dimitrakopulos, G. P. & Karakostas, Th. (1996). *Acta Cryst.* A**52**, 62–76.
Gertsman, V. Y. (2001). *Acta Cryst.* A**57**, 369–377.
Gertsman, V. Y. & Bruemmer, S. M. (2001). *Acta Mater.* **49**, 1589–1598.
Gertsman, V. Y. & Szpunar, J. A. (1998). *Scr. Mater.* **38**, 1399–1404.
Grimmer, H., Bollmann, W. & Warrington, D. H. (1974). *Acta Cryst.* A**30**, 197–207.
King, A. H. (1999). *Interface Sci.* **7**, 251–271.
Kopezky, C. V., Andreeva, A. V. & Sukhomlin, G. D. (1991). *Acta Metall. Mater.* **39**, 1603–1615.
Miyazawa, K., Iwasaki, Y., Ito, K. & Ishida, Y. (1996). *Acta Cryst.* A**52**, 787–796.
Palumbo, G., Aust, K. T., Erb, U., King, P. J., Brennenstuhl, A. M. & Lichtenberger, P. C. (1992). *Phys. Status Solidi A*, **131**, 425–428.
Watanabe, T. (1984). *Res. Mech.* **11**, No. 11, 47–84.